

USPR: Learning a Unified Solver for Profiled Routing

Chuanbo Hua^{*,1,2}, Federico Berto^{*,1,2}, Zhikai Zhao¹, Jiwoo Son², Changhyun Kwon^{1,2} and Jinkyoo Park^{1,2}

¹KAIST ²OMELET AI4CO[†]

Abstract. The Profiled Vehicle Routing Problem (PVRP) extends the classical VRP by incorporating vehicle-client-specific preferences and constraints, reflecting real-world requirements such as zone restrictions and service-level preferences. While recent reinforcement-learning (RL) solvers have shown promise, they require retraining for each new profile distribution, suffer from poor representation ability, and struggle to generalize to out-of-distribution instances. In this paper, we address these limitations by introducing USPR (Unified Solver for Profiled Routing), a novel framework that natively handles arbitrary profile types. USPR introduces three key innovations: (i) Profile Embeddings (PE) to encode any combination of profile types; (ii) Multi-Head Profiled Attention (MHPA), an attention mechanism that models rich interactions between vehicles and clients; (iii) Profile-aware Score Reshaping (PSR), which dynamically adjusts decoder logits using profile scores to improve generalization. Empirical results on diverse PVRP benchmarks demonstrate that USPR achieves state-of-the-art results among learning-based methods while offering significant gains in flexibility and computational efficiency. We make our source code publicly available to foster future research at <https://github.com/ai4co/uspr>.

1 Introduction

The Vehicle Routing Problem (VRP) is an important combinatorial optimization problem that focuses on determining optimal delivery routes for a fleet of vehicles serving a set of clients. In real-world logistics operations, vehicles often have distinct characteristics that affect their suitability for serving specific clients, leading to the Profiled Vehicle Routing Problem (PVRP). This variant extends traditional VRP constraints by incorporating vehicle-client-specific preferences and operational requirements [12, 10, 68, 1]. These profiles can represent various practical considerations: specialized vehicle access permissions in urban areas, client-specific service level agreements, regulatory restrictions, or historical performance metrics that influence routing decisions [57, 37]. For instance, in last-mile delivery scenarios, certain vehicles might be preferred for specific neighborhoods based on size restrictions or noise regulations, while in B2B logistics, particular vehicle-driver combinations might maintain stronger relationships with certain clients. Fig. 1 provides a visualization for the PVRP problem. The PVRP's inherent complexity stems from its NP-hard nature, as it generalizes the classical VRP while adding profile-specific constraints that exponentially increase the solution space [47, 17]. This complexity becomes particularly challenging in modern logistics operations, where organizations must

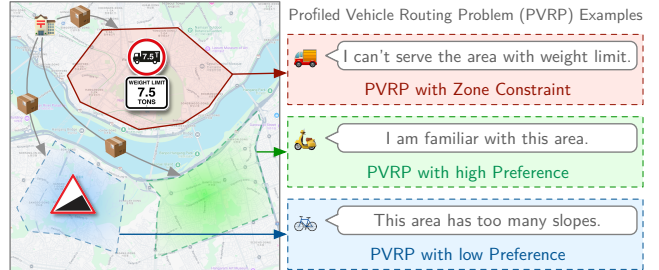


Figure 1. PVRP with profiles based on constraints and preferences.

optimize routes for large fleets while considering numerous client-specific requirements and dynamically changing preferences.

Traditional approaches to solving PVRP typically rely on exact methods like Branch and Bound for small instances or metaheuristic algorithms such as genetic algorithms and simulated annealing for larger problems [26, 43]. While these methods can provide optimal or near-optimal solutions, they often require significant computational resources and extensive parameter tuning. Moreover, these approaches generally need to be redesigned or substantially modified when problem specifications change, such as when new types of preferences or constraints are introduced. This lack of adaptability poses a significant challenge in dynamic business environments where routing requirements frequently evolve.

Recent advances in neural combinatorial optimization, particularly through reinforcement learning (RL), have shown promising results for various VRP variants [3, 54]. These approaches leverage neural architectures, especially the pointer network paradigm [60, 31, 15], to learn solution strategies through interaction with simulated environments. While initial work focused on basic VRP variants [33, 28, 67], recent studies have extended these methods to handle more complex scenarios, including multi-agent routing [70], rich constrained variants [40, 69, 8], and heterogeneous fleet problems extensible to the PVRP [35, 42, 5, 24].

However, existing learning-based PVRP solvers exhibit three major shortcomings. First, they must be retrained from scratch whenever the profile distribution or preference weights change, incurring prohibitive computational overhead. Second, they lack the representational capacity to capture complex vehicle-client interactions, leading to suboptimal embeddings and degraded solution quality. Third, they generalize poorly to out-of-distribution instances, making them fragile in dynamic or unseen settings. Together, these issues undermine the flexibility and efficiency required for real-world deployment of neural routing methods.

To bridge these limitations, we introduce USPR (Unified Solver for Profiled Routing), a single transformer-based policy that unifies vehicle-client profiles and directly addresses the three core short-

^{*} Equal contribution.

[†] Work made with contributions from the AI4CO open research community.

comings of existing methods: (i) Profile Embeddings (PE) encode arbitrary combinations of profile attributes and global weight parameters, removing the need to retrain for each new profile distribution; (ii) Multi-Head Profiled Attention (MHPA) overcomes weak representation by capturing rich, bidirectional vehicle–client interactions; and (iii) Profile-aware Score Reshaping (PSR) adaptively reweights decoder logits with profile scores and spatial penalties, yielding robust generalization to out-of-distribution instances.

We summarize our contributions as follows:

- We introduce USPR, a novel method for learning unified neural solvers for the PVRP.
- We introduce Profile Embeddings (PE) to project any combination of profile attributes and global weight parameters into a shared latent space, allowing adaptation to new profile distributions without retraining.
- We design Multi-Head Profiled Attention (MHPA) to capture rich, bidirectional interactions between every vehicle and client, greatly enhancing representational capacity.
- We propose Profile-Aware Score Reshaping (PAR) to dynamically reweight decoder logits by integrating profile scores with spatial penalties, ensuring robust performance on out-of-distribution instances.
- We validate our approach across diverse PVRP benchmarks, showing that a single USPR model outperforms existing learning-based methods in solution quality while reducing model size and training times by an order of magnitude.

2 Related Work

Neural Combinatorial Optimization Neural combinatorial optimization (NCO) has emerged as a powerful paradigm for solving vehicle routing problems (VRPs), offering promising end-to-end solutions that reduce the need for manual algorithm design [4, 6, 45, 39]. The field was pioneered by Vinyals et al. [60], Bello et al. [3] with Pointer Networks. These methods were significantly advanced by Kool et al. [31]’s seminal work, which introduced a transformer-based architecture trained via RL for solving VRPs, which remains the de facto basis for most modern neural VRP approaches. Recent developments in NCO for VRPs can be broadly categorized into construction and improvement methods. Construction methods [28, 9, 18, 50, 65] focus on generating solutions from scratch, while improvement/search methods [20, 36, 38, 44, 46] iteratively refine existing solutions. Construction approaches have seen significant innovations, including non-autoregressive methods [32, 53] that predict promising edges simultaneously, and population-based approaches [19, 22] that maintain solution diversity. These have been complemented by advances in training strategies, such as problem re-encoding [2, 13] and test-time adaptation & search [21, 11, 27, 29, 63, 23]. In this work, we focus on construction approaches for VRPs because of their adaptability to various settings and advantageous solution quality and inference time tradeoff.

NCO for Practical VRPs As NCO methods mature, there is increasing focus on addressing “in the wild” VRPs – VRP variants with complex constraints and real-world desiderata that can be applied in practical scenarios. Duan et al. [15], Son et al. [52] explore the gap between synthetic Euclidean and real-world asymmetric topological settings by modeling data distributions. Several works have extended to multiple complex constraints [8, 40] with several multi-task learning methods [14, 40, 69, 7, 34, 16]. An important practical direction to model multiple vehicles in restricted numbers – a realistic setting which most previous approaches do not consider – has

tackled multi-agent scenarios via multi-agent RL [70] and one-agent-at-a-time autoregressive reformulations [51, 67]. Some recent works tackle the setting of both limited vehicles and heterogeneous fleets modeling different vehicles [35, 5], which are recently extended to handle the more practical PVRPs [24] that models not only different vehicle entities but also different vehicle-node interactions, i.e. *profiles*, in terms of preferences of varying magnitudes and zone constraints. Despite recent progress, neural VRP solvers still struggle with weak profile modeling, require retraining for each new preference or constraint, and generalize poorly to unseen scenarios, which this work aims to solve.

3 Preliminaries

We introduce the problem formulation of the PVRP in Section 3.1, its MDP equivalent in Section 3.2, and the policy parametrization in Section 3.3.

3.1 Problem Formulation

We consider a directed graph $G = (V, E)$, where $V = \{0, \dots, N\}$ is the set of nodes, including $\{0\}$ as the depot and $\{1, \dots, N\}$ as clients, and vehicle set $K = \{1, \dots, M\}$ is the set of vehicles. Each client $i \in N$ has demand d_i , and each vehicle $k \in K$ has capacity Q_k , speed v_k , and a profile score $p_{ik} \in \mathbb{R} \cup \{-\infty\}$. Intuitively, a higher profile score means that vehicle k is encouraged to serve client i ; symmetrically, this could also be understood as client i preferring vehicle k to serve them. If the profile score is $-\infty$, it means a hard constraint, i.e., the vehicle k can not serve the client i . The edges E connect pairs of nodes, and each edge $(i, j) \in E$ has a travel distance c_{ij} . We introduce the decision variables $x_{ij}^k = 1$ if vehicle k travels from i to j (and 0 otherwise) and $y_i^k = 1$ if vehicle k serves client i (and 0 otherwise). The objective is to maximize total profile reward minus travel time, balanced via a profile weight $\alpha \in [0, 1]$:

$$\max_{x, y} \sum_{k \in K} \sum_{i \in V} \sum_{j \in V} (\alpha p_{ik} - \frac{c_{ij}}{v_k}) x_{ij}^k. \quad (1)$$

Subject to:

$$\sum_{k \in K} y_i^k = 1 \quad \forall i \in N, \quad (1a)$$

$$\sum_{i \in N} \sum_{j \in V} d_i x_{ij}^k \leq Q_k \quad \forall k \in K, \quad (1b)$$

$$\sum_{j \in V} x_{hj}^k = \sum_{i \in V} x_{ih}^k \quad \forall h \in V, k \in K, \quad (1c)$$

$$x_{ij}^k \in \{0, 1\}, \quad y_i^k \in \{0, 1\} \quad \forall i, j \in V, k \in K. \quad (1d)$$

Constraint (1a) ensures each client is served once, (1b) enforces vehicle capacities, (1c) preserves route continuity and prevents subtours, and (1d) enforces integrality (i.e. decision variables must be binary values). By setting all $p_{ik} = 0$, we recover the classical VRP⁰; allowing positive $p_{ik} \in \mathbb{R}^+$ encodes client–vehicle affinities – i.e., PVRP-P for *preferences*, while $p_{ik} = -\infty$ forbids the assignment of vehicle k to client i – i.e. PVRP-ZC for *zone constraints*.

⁰ Specifically, this case would be a Capacitated Vehicle Routing Problem (CVRP) where the objective is to minimize the total travel time (duration).

3.2 MDP Formulation

The PVRP can be naturally framed as a Markov Decision Process (MDP), which enables the application of Reinforcement Learning (RL) techniques for scalable and adaptive solution generation [24]. We define the MDP formulation as follows:

State Space (\mathcal{S}) A state $s_t \in \mathcal{S}$ at time step t captures the partial route constructed up to that point. This includes the current location of all vehicles $s_n \in \mathbb{R}^2$, the remaining capacity Q_m^t of each vehicle $m \in \mathcal{M}$, the set of visited and unvisited clients, the client-vehicle profile matrix P_m , and the accumulated travel cost. The state representation provides a complete view of the system's current configuration.

Action Space (\mathcal{A}) At each decision step, an action consists of selecting which client to visit next or returning to the depot. The action space encompasses all unvisited clients $n \in \mathcal{N}$ that satisfy capacity constraints and zone restrictions for the current vehicle, as well as the option to return to the depot to initialize a new route segment when necessary.

Transition Dynamics (\mathcal{T}) The system evolves according to a deterministic transition function $s_{t+1} = \mathcal{T}(s_t, a_t)$, which updates vehicle locations, remaining capacities, and the set of visited clients based on the selected action. When a vehicle visits a client, the client's demand is subtracted from the vehicle's capacity, and the client is marked as served. If a vehicle returns to the depot, its capacity is reset to the initial value, enabling it to start a new route segment.

Reward Function (\mathcal{R}) To align with the bi-objective nature of PVRP, we define the reward for each action as $r_t = \alpha p_{nm} - c_{ij}/v_m$ as per Eq. (1), where p_{nm} represents the client-vehicle preference score, c_{ij}/v_m accounts for the travel cost, and α controls the trade-off between preference satisfaction and transportation efficiency. In practice, we employ a sparse reward strategy, calculating the cumulative reward efficiently at the end of each episode (i.e., when solution construction completes at time T): this approach is equivalent to using the unified objective defined in the problem formulation. Throughout the paper, we use the notation $R(\mathbf{x}, \mathbf{a}, \alpha)$ to represent the reward function \mathcal{R} that generates a signal given an instance \mathbf{x} , a complete solution \mathbf{a} , and its corresponding α .

Policy (π) A policy $\pi(a_t|s_t)$ specifies the probability distribution over possible actions given the current state. Our objective is to learn an optimal policy π^* that maximizes the expected cumulative reward:

$$\pi^* = \arg \max_{\pi} \mathbb{E} \left[\sum_{t=0}^T \gamma^t r_t \right] \quad (2)$$

where $\gamma \in [0, 1]$ is a discount factor which we set to 1 (i.e., effectively no discounting) due to the sparse nature of our reward signal.

3.3 Policy Parameterization

To generate solutions efficiently, we employ parallel autoregressive models for policy learning [5, 24] with an encoder-decoder framework. The encoder network $f_{\theta}(\mathbf{x}, \alpha)$ processes problem instance \mathbf{x} and profile weight α into a structured representation \mathbf{h} . At each step t , the decoder network g_{θ} generates a joint action vector $\mathbf{a}_t = (a_t^1, \dots, a_t^M)$ for all M vehicles. The policy π_{θ} is defined as:

$$\pi_{\theta}(\mathbf{a}|\mathbf{x}, \alpha) = \prod_{t=1}^T \psi \left(\prod_{k=1}^M g_{\theta}(a_t^k | \mathbf{a}_{t-1}, \mathbf{a}_{t-2}, \dots, \mathbf{a}_1, \mathbf{h}) \right) \quad (3)$$

where ψ is a conflict resolution function that ensures solution feasibility by prioritizing assignments to the agent with the largest log-probability value.

4 Methodology

We now present our proposed USPR framework as illustrated in Fig. 2. We introduce three key components for unified profile handling: Profile Embeddings (PE, Section 4.1), Multi-Head Profiled Attention (MHPA, Section 4.2), and Profile-aware Score Reshaping (PSR, Section 4.3). Together, these components enable flexible adaptation to different profile weights and problem settings within a single model architecture. We then lay out the integration into the encoder-decoder framework (Section 4.4) and the training scheme (Section 4.5).

4.1 Profile Embeddings

Previous approaches handle profiles by retraining separate models for each profile distribution, which is computationally inefficient and lacks flexibility. Our Profile Embeddings (PE) overcome this limitation by learning a unified representation that can encode any combination of attributes and profile weight parameters. Given an instance \mathbf{x} and corresponding profile weight parameter α , we first embed these features into a latent space \mathbf{h} of size d_h by considering separated contributions for clients, vehicles, profiles, and profile weights via linear layers parametrized by matrices $\mathbf{W}_{\text{init}}^{(\cdot)}$ and bias vectors $\mathbf{b}_{\text{init}}^{(\cdot)}$.

Client Feature Embeddings project client-specific information into a latent space:

$$\mathbf{h}_i^c = \mathbf{W}_{\text{init}}^c \mathbf{x}_i^c + \mathbf{b}_{\text{init}}^c \in \mathbb{R}^{d_h} \quad (4)$$

where $\mathbf{x}_i^c \in \mathbb{R}^{d_c}$ contains client-specific features including demands and locations of size d_c , $\mathbf{W}_{\text{init}}^c \in \mathbb{R}^{d_h \times d_c}$, and $\mathbf{b}_{\text{init}}^c \in \mathbb{R}^{d_h}$.

Vehicle Feature Embeddings project vehicle-specific information:

$$\mathbf{h}_j^v = \mathbf{W}_{\text{init}}^v \mathbf{x}_j^v + \mathbf{b}_{\text{init}}^v \in \mathbb{R}^{d_h} \quad (5)$$

where $\mathbf{x}_j^v \in \mathbb{R}^{d_v}$ contains vehicle-specific features of size d_v including capacity and starting location, which practically encodes the depot information, $\mathbf{W}_{\text{init}}^v \in \mathbb{R}^{d_h \times d_v}$, and $\mathbf{b}_{\text{init}}^v \in \mathbb{R}^{d_h}$.

Profile Score Embeddings transform raw profile scores into learnable embeddings:

$$\mathbf{h}_{ij}^p = \mathbf{W}_{\text{init}}^p p_{ij} + \mathbf{b}_{\text{init}}^p \in \mathbb{R}^{d_h} \quad (6)$$

where $p_{ij} \in \mathbb{R}$ represents the profile between vehicle i and client j , $\mathbf{W}_{\text{init}}^p \in \mathbb{R}^{d_h \times 1}$, and $\mathbf{b}_{\text{init}}^p \in \mathbb{R}^{d_h}$.

Profile Weight Embeddings encode objective weights to enable flexible tradeoffs:

$$\mathbf{h}^{\alpha} = \mathbf{W}_{\text{init}}^{\alpha} \alpha + \mathbf{b}_{\text{init}}^{\alpha} \in \mathbb{R}^{d_h} \quad (7)$$

where $\alpha \in \mathbb{R}$ represents the profile weights from Eq. (1) which are then broadcasted on other embeddings, $\mathbf{W}_{\text{init}}^{\alpha} \in \mathbb{R}^{d_h \times 1}$, and $\mathbf{b}_{\text{init}}^{\alpha} \in \mathbb{R}^{d_h}$. PEs create a shared latent space that enables the model to handle arbitrary profile types without retraining. By projecting the client, vehicle, profiles, and profile weights, the model can simultaneously process profiles with varying magnitudes and values.

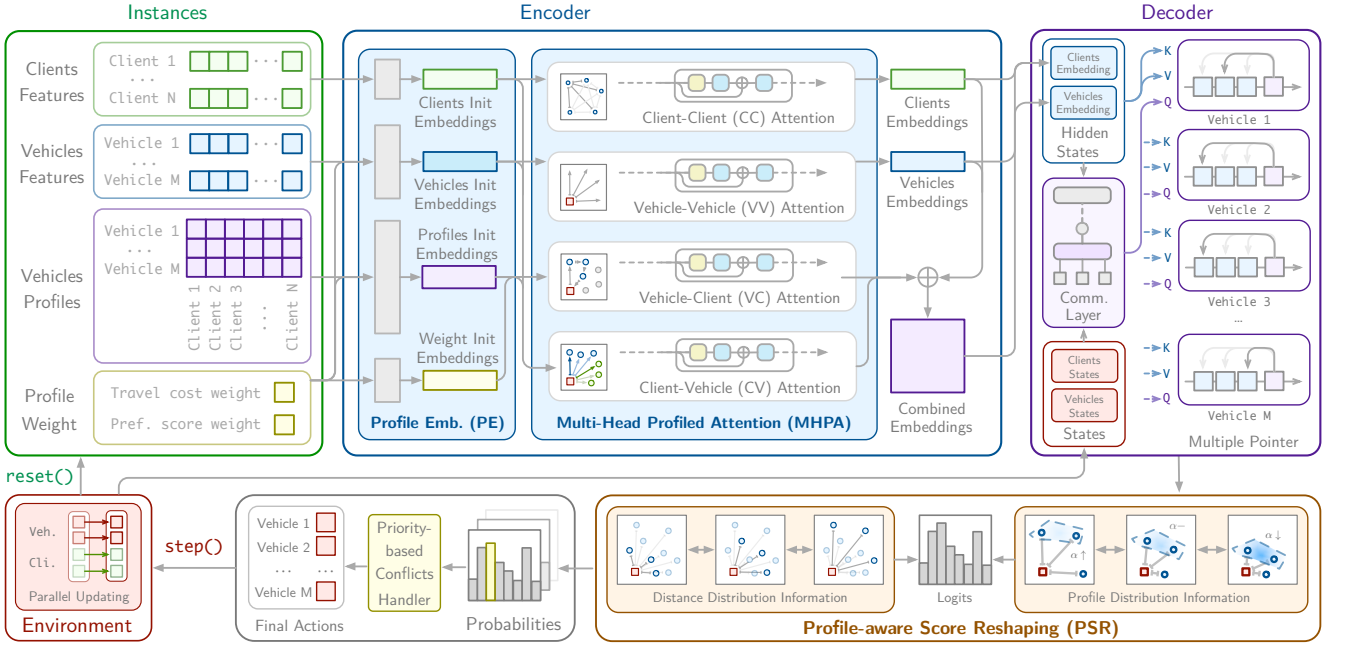


Figure 2. Overview of our USPR.

4.2 Multi-Head Profiled Attention

A fundamental limitation of existing approaches is their inability to capture rich bidirectional interactions between vehicles and clients with different profiles. To address this, we introduce Multi-Head Profiled Attention (MHPA) to allow for improved information exchange in each encoder layer:

$$\mathbf{h} = \text{Norm}(\text{MHPA}(\mathbf{h})) \quad (8)$$

$$\mathbf{h} = \text{Norm}(\text{FFN}(\mathbf{h}) + \mathbf{h}) \quad (9)$$

where FFN denotes a multi-layer perceptron. MHPA is based on multi-head attention (MHA):

$$\text{MHA}(\mathbf{Q}, \mathbf{K}, \mathbf{V}) = \left(\parallel_{i=1}^{n_{\text{heads}}} \text{Attention}(\mathbf{Q}\mathbf{W}_i^Q, \mathbf{K}\mathbf{W}_i^K, \mathbf{V}\mathbf{W}_i^V) \right) \mathbf{W}^O \quad (10)$$

with

$$\text{Attention}(\mathbf{Q}, \mathbf{K}, \mathbf{V}) = \text{softmax} \left(\frac{\mathbf{Q}\mathbf{K}^T}{\sqrt{d_h}} \right) \mathbf{V} \quad (11)$$

MHPA improves on MHA for modeling PVRP with four distinct types of information exchange depending on the embedding:

1) *Client-Client (CC) Attention* enables information sharing between clients about their spatial relationships and demands:

$$\mathbf{h}^c' = \text{MHA}(\mathbf{h}^c, \mathbf{h}^c, \mathbf{h}^c) \quad (12)$$

2) *Vehicle-Vehicle (VV) Attention* facilitates communication between vehicles about their capacities and service capabilities:

$$\mathbf{h}^v' = \text{MHA}(\mathbf{h}^v, \mathbf{h}^v, \mathbf{h}^v) \quad (13)$$

3) *Vehicle-Client (VC) Attention* enables vehicles to attend to relevant clients based on profiles:

$$\mathbf{h}_i^{pv'} = \text{MHA}(\mathbf{h}^v, \mathbf{h}^c, \mathbf{h}_i^{pv}) \quad (14)$$

4) *Client-Vehicle (CV) Attention* allows clients to consider their suitability for different vehicles based on their profiles:

$$\mathbf{h}_i^{pv'} = \text{MHA}(\mathbf{h}^c, \mathbf{h}^v, \mathbf{h}_i^{pc}) \quad (15)$$

Unlike previous approaches that only consider unidirectional interactions or simple aggregations, MHPA enables comprehensive information exchange through bidirectional attention mechanisms. The final MHPA output integrates all processed information:

$$\mathbf{h}_{ij}^{p'} = \text{concat}(\mathbf{h}_i^v, \mathbf{h}_j^c, \mathbf{h}_i^{pv'}, \mathbf{h}_j^{pc'}) + \mathbf{h}_{ij}^p \quad (16)$$

where each vehicle is assigned its own \mathbf{h} processed latent representation.

4.3 Profile-aware Score Reshaping

We further introduce Profile-aware Score Reshaping (PSR), which dynamically adjusts decoder logits to maintain robustness across varying profile distributions and out-of-distribution instances. Building on recent advancements in distance-based heuristics [61, 25], PSR further combines learned embeddings with explicit profile and distance information:

$$\mathbf{Z} = C \cdot \tanh \left(\frac{\mathbf{U}(\mathbf{W}_{\text{ptr}} \mathbf{h})^T - \log(\text{dist}_{ij} + p_{ij})}{\sqrt{d_h}} \right) \quad (17)$$

where C is a scaling factor set to 10 following Bello et al. [3], $\mathbf{U} \in \mathbb{R}^{M \times d_h}$ represents the decoder's query vectors, \mathbf{W}_{ptr} projects node embeddings into the pointer space, dist_{ij} is the distance between nodes i and j , and p_{ij} is the preference score between vehicle i and client j ¹.

PSR provides several key advantages: it balances the flexibility of neural approaches with the reliability of traditional heuristics; naturally penalizes nodes that are either spatially distant or have low preference scores; ensures consistent performance across varying profile

¹ We note that while we manually design the attention reshaping mechanism in this paper, we could leverage automatic algorithm design [41, 64, 49, 58, 66] to do it, which we leave as future work.

distributions and out-of-distribution instances; and enables smooth adaptation without retraining when preference weights change. The final action probabilities are computed by masking infeasible actions and applying softmax:

$$P(\mathbf{a}_t | \mathbf{s}_t) = \text{softmax}(\mathbf{Z} + \mathbf{M}_t) \quad (18)$$

where \mathbf{M}_t is the mask tensor for infeasible actions at step t .

4.4 Integration into Encoder-Decoder Framework

The three components described above are integrated into an encoder-decoder framework [24]. The encoder $f_\theta(\mathbf{x}, \alpha)$ first processes raw problem features using PE to create initial embeddings as in Section 4.1, then applies encoder layers with MHPA from Section 4.2 to capture complex interactions between clients and vehicles. The encoder outputs a set of embeddings $\mathbf{h} = [\mathbf{h}^1, \dots, \mathbf{h}^M]$, where each $\mathbf{h}^k \in \mathbb{R}^{(M+N) \times d_h}$ represents the encoded graph information for vehicle profile k .

The decoder g_θ generates vehicle-specific queries that capture both profile and current state information:

$$\mathbf{q}_t^k = \mathbf{W}_{\text{query}}[\mathbf{h}_k^k \| \mathbf{h}_{\text{cur}}^k \| \mathbf{W}_{\text{state}} \mathbf{s}_t^k] \quad (19)$$

where $\|\cdot\|$ denotes concatenation, \mathbf{h}_k^k is the vehicle's profile embedding, $\mathbf{h}_{\text{cur}}^k$ represents the current node embedding, and \mathbf{s}_t^k captures the state features at time t . We then process the multiple vehicle queries $\mathbf{q}_t = [\mathbf{q}_t^1, \dots, \mathbf{q}_t^M]$ via a single communication layer [5, 24] – common also outside of VRPs [55, 56] – composed of standard MHA and FFN, and then these are fed into a multiple pointer mechanism that generates the decoder output \mathbf{U} . Finally, PSR is applied to compute action probabilities for each vehicle as in Section 4.3.

4.5 Training

We train our model using the REINFORCE algorithm with a shared baseline [28] across all agents. During training, we sample α_i from a predefined distribution of profile weights $\mathcal{D}_\alpha = [\alpha_{\min}, \alpha_{\max}]$ for each instance in the batch. This allows the model to learn a unified policy across different preference-cost trade-offs.

The policy gradient is estimated as:

$$\nabla_\theta \mathcal{L} = \frac{1}{B \cdot L} \sum_{i=1}^B \sum_{j=1}^L (R(\mathbf{x}_i, \mathbf{a}_{ij}, \alpha_i) - b^{\text{shared}}(\mathbf{x}_i)) \cdot \nabla_\theta \log p_\theta(\mathbf{a}_{ij} | \mathbf{x}_i, \alpha_i) \quad (20)$$

where B is the batch size, L is the number of solutions per instance, and b^{shared} is the shared baseline value obtained through symmetric augmentation sampling.

5 Experiments

We evaluate the effectiveness of our approach with comprehensive experiments in various settings, including in-distribution performance analysis, large-scale (out-of-distribution) generalization analysis, real-world application, model components ablation study, and further analyses. We compare USPR against both classical and learning-based baselines.

5.1 Experimental Setup

Code Our code is written in PyTorch using RL4CO [6]. We are committed to releasing the source code and models upon acceptance to foster academic research. All training and testing are run on an AMD Ryzen Threadripper 3960X (24-core) CPU with an NVIDIA RTX 4090 GPU.

Data Generation We generate synthetic PVRP instances by sampling client and depot coordinates $(x_i, y_i) \sim \text{Uniform}(0, 1)$ for $i = 0, 1, \dots, N$, where $i = 0$ denotes the depot, and drawing client demands $d_i \sim \text{UniformInteger}(1, 9)$ for $i = 1, \dots, N$. We use $M = 7$ and $N = 100$ in the main experiments. Each of the M vehicles has capacity $Q_k = 40$ and speed $v_k = 1$, so that Euclidean distance equals travel time. For the preference-based variant (VRP-P), profile scores are drawn as $p_{ik} \sim \text{Uniform}(0, 1)$ independently for all client–vehicle pairs. For the zone-constrained variant (VRP-ZC), we partition the service area into $S = M$ angular sectors, sample a constraint rate $r \sim \text{Uniform}(0, \frac{2}{3})$, and for each client i randomly mask $\lfloor rS \rfloor$ sectors; vehicles whose home sector is masked for client i are assigned $p_{ik} = -\infty$, forbidding those assignments.

Classical Baselines We employ two state-of-the-art classical solvers: Google OR-Tools [48], a versatile framework that combines exact and heuristic methods via constraint programming, and HGS-PyVRP [62], an open-source implementation of the Hybrid Genetic Search for the CVRP [59] that supports the PVRP. We handle vehicle-specific profiles by modifying the cost matrices for each vehicle according to the objective function in Eq. (1).

Neural Baselines We compare against several recent neural VRP solvers: ET [51], which specializes in sequential multi-agent routing with equitable workload distribution; DPN [67], which enhances ET with an improved encoder for route partitioning; 2D-Ptr [42], which uses dual encoding for dynamic adaptation in heterogeneous routing; and PARCO [5], which employs parallel decoding with inter-agent communication; and CAMP [24], which was specifically designed for PVRP. Since ET, DPN, 2D-Ptr, and PARCO do not natively handle client–vehicle profiles, we adapt them by concatenating profile-specific features (client–vehicle preference scores and zone-constraint indicators) into both their initial node embeddings and the decoder's context embeddings at each step. CAMP already incorporates profiled client embeddings and inter-agent communication, so no further modification is needed.

Training Configuration All models are trained under identical settings to ensure a fair comparison. We optimize using Adam [30] with an initial learning rate of 10^{-4} , decaying by a factor of 0.1 at epochs 80 and 95. Training runs for 100 epochs with 10^5 samples per epoch, using a batch size of 32 and 8 augmented rollouts via Sym-NCO [28] per instance for baseline estimation. Architecturally, each model employs $d_h = 128$ hidden-dimensional embeddings, 8 attention heads, and 512-dimensional feedforward layers across 3 encoder layers. For baseline models, we train a separate model for each fixed α taken from $\alpha \in \{0.00, 0.025, \dots, 0.20\}$ and zone constraint (10 models in total), where the final reported performance for PVRP-P is the average of results across all α values. As a unified model, USPR is trained in a mixed profile way: at each training step, we uniformly sample the number of clients $N \in \{60, \dots, 100\}$ and vehicles $M \in \{3, \dots, 7\}$, profile weights α range from $\alpha_{\min} = 0$ to $\alpha_{\max} = 0.2$, also including a sampling probability for the zone-constraint of 10%. Thus, USPR trains a single unified model by sampling α uniformly from this set at every step.

Table 1. Benchmarks and results for PVRP-P (top) and PVRP-ZC (bottom) at varying sizes and agent numbers. Highlighting cost (\downarrow) and average gaps (\downarrow) to the sota HGS-PyVRP. Single instance solution time in parentheses.

PVRP-P (Preferences)											
<i>N</i>	60			80			100			Gap(%)	
<i>M</i>	3	5	7	3	5	7	3	5	7	avg.	
OR-Tools	7.34 (10m)	7.64 (10m)	7.87 (10m)	8.42 (12m)	9.02 (12m)	9.19 (12m)	10.15 (15m)	10.32 (15m)	10.62 (15m)	10.68	
	6.44 (10m)	6.83 (10m)	7.10 (10m)	7.66 (12m)	8.17 (12m)	8.47 (12m)	8.93 (15m)	9.50 (15m)	9.80 (15m)	0.00	
ET (g.)	7.62 (0.17s)	8.12 (0.17s)	8.41 (0.18s)	9.04 (0.23s)	9.63 (0.24s)	9.96 (0.23s)	10.50 (0.28s)	11.18 (0.30s)	11.63 (0.30s)	18.13	
DPN (g.)	7.52 (0.17s)	8.00 (0.18s)	8.27 (0.18s)	8.93 (0.22s)	9.63 (0.24s)	10.05 (0.24s)	10.50 (0.29s)	11.08 (0.29s)	11.42 (0.30s)	17.15	
2D-Ptr (g.)	7.34 (0.15s)	7.75 (0.15s)	8.03 (0.16s)	8.70 (0.20s)	9.30 (0.19s)	9.59 (0.20s)	10.10 (0.25s)	10.82 (0.25s)	11.18 (0.25s)	13.86	
PARCO (g.)	7.31 (0.14s)	7.73 (0.15s)	8.08 (0.15s)	8.69 (0.21s)	9.19 (0.22s)	9.57 (0.22s)	10.14 (0.25s)	10.78 (0.24s)	11.10 (0.25s)	13.21	
CAMP (g.)	7.16 (0.17s)	7.66 (0.18s)	7.88 (0.18s)	8.49 (0.25s)	9.07 (0.25s)	9.44 (0.25s)	9.87 (0.33s)	10.60 (0.33s)	10.90 (0.33s)	11.23	
USPR (g.)	7.13 (0.10s)	7.56 (0.11s)	7.86 (0.11s)	8.48 (0.14s)	9.03 (0.14s)	9.37 (0.15s)	9.87 (0.18s)	10.47 (0.20s)	10.82 (0.22s)	10.51	
ET (s.)	7.16 (0.25s)	7.62 (0.24s)	7.87 (0.25s)	8.51 (0.35s)	9.05 (0.37s)	9.41 (0.36s)	9.93 (0.45s)	10.55 (0.44s)	10.88 (0.46s)	11.23	
DPN (s.)	7.13 (0.27s)	7.55 (0.26s)	7.87 (0.26s)	8.46 (0.34s)	9.04 (0.37s)	9.36 (0.36s)	9.85 (0.43s)	10.52 (0.42s)	10.88 (0.48s)	10.69	
2D-Ptr (s.)	6.89 (0.16s)	7.31 (0.17s)	7.57 (0.17s)	8.23 (0.20s)	8.72 (0.21s)	9.09 (0.22s)	9.57 (0.26s)	10.14 (0.26s)	10.45 (0.27s)	6.81	
PARCO (s.)	6.87 (0.21s)	7.25 (0.23s)	7.55 (0.22s)	8.13 (0.33s)	8.66 (0.35s)	9.02 (0.34s)	9.44 (0.42s)	10.12 (0.41s)	10.49 (0.41s)	6.44	
CAMP (s.)	6.75 (0.33s)	7.18 (0.35s)	7.45 (0.33s)	8.05 (0.43s)	8.57 (0.42s)	8.90 (0.42s)	9.38 (0.51s)	9.96 (0.54s)	10.29 (0.54s)	5.02	
USPR (s.)	6.73 (0.20s)	7.13 (0.22s)	7.41 (0.23s)	8.00 (0.31s)	8.53 (0.33s)	8.84 (0.34s)	9.33 (0.40s)	9.92 (0.42s)	10.24 (0.43s)	4.42	
PVRP-ZC (Zone Constraints)											
<i>N</i>	60			80			100			Gap(%)	
<i>M</i>	3	5	7	3	5	7	3	5	7	avg.	
OR-Tools	13.17 (10m)	13.15 (10m)	13.18 (10m)	16.67 (12m)	16.69 (12m)	16.70 (12m)	20.18 (15m)	20.22 (15m)	20.20 (15m)	8.35	
	12.13 (10m)	12.16 (10m)	12.16 (10m)	15.36 (12m)	15.40 (12m)	15.42 (12m)	18.59 (15m)	18.66 (15m)	18.70 (15m)	0.00	
ET (g.)	13.87 (0.17s)	14.04 (0.17s)	13.91 (0.17s)	17.55 (0.23s)	17.54 (0.23s)	17.48 (0.24s)	21.28 (0.28s)	21.20 (0.29s)	21.36 (0.29s)	14.15	
DPN (g.)	13.98 (0.17s)	13.94 (0.17s)	13.81 (0.17s)	17.50 (0.22s)	17.62 (0.22s)	17.57 (0.23s)	21.24 (0.28s)	21.31 (0.28s)	21.37 (0.28s)	14.14	
2D-Ptr (g.)	13.42 (0.15s)	13.49 (0.15s)	13.37 (0.15s)	16.98 (0.20s)	16.95 (0.20s)	17.04 (0.20s)	20.53 (0.25s)	20.58 (0.24s)	20.57 (0.25s)	10.06	
PARCO (g.)	13.39 (0.14s)	13.42 (0.13s)	13.32 (0.13s)	16.87 (0.21s)	16.95 (0.20s)	16.82 (0.20s)	20.33 (0.25s)	20.52 (0.25s)	20.33 (0.25s)	9.55	
CAMP (g.)	12.93 (0.19s)	13.07 (0.20s)	13.14 (0.18s)	16.59 (0.25s)	16.38 (0.25s)	16.52 (0.24s)	20.00 (0.33s)	20.18 (0.32s)	20.07 (0.33s)	7.62	
USPR (g.)	12.61 (0.09s)	12.55 (0.10s)	12.56 (0.10s)	15.90 (0.12s)	15.83 (0.13s)	15.86 (0.13s)	19.26 (0.15s)	19.30 (0.17s)	19.37 (0.19s)	7.31	
ET (s.)	13.18 (0.25s)	13.17 (0.25s)	13.18 (0.25s)	16.63 (0.34s)	16.73 (0.34s)	16.58 (0.34s)	20.19 (0.46s)	20.47 (0.45s)	20.14 (0.45s)	8.78	
DPN (s.)	13.13 (0.27s)	13.30 (0.27s)	13.24 (0.26s)	16.62 (0.33s)	16.67 (0.33s)	16.78 (0.34s)	20.23 (0.44s)	20.18 (0.44s)	20.34 (0.43s)	8.69	
2D-Ptr (s.)	12.86 (0.15s)	12.93 (0.15s)	12.99 (0.15s)	16.33 (0.21s)	16.31 (0.21s)	16.17 (0.22s)	19.76 (0.25s)	19.72 (0.25s)	19.90 (0.25s)	5.92	
PARCO (s.)	12.85 (0.21s)	12.81 (0.22s)	12.86 (0.22s)	16.28 (0.33s)	16.46 (0.33s)	16.31 (0.33s)	19.64 (0.42s)	19.72 (0.42s)	19.79 (0.41s)	5.86	
CAMP (s.)	12.54 (0.33s)	12.50 (0.33s)	12.52 (0.34s)	15.77 (0.42s)	15.84 (0.43s)	15.88 (0.42s)	19.06 (0.50s)	19.26 (0.49s)	19.18 (0.49s)	3.31	
USPR (s.)	12.41 (0.17s)	12.41 (0.18s)	12.42 (0.20s)	15.71 (0.25s)	15.73 (0.28s)	15.72 (0.29s)	19.00 (0.35s)	19.14 (0.36s)	19.18 (0.37s)	3.12	

Table 2. Benchmarks and generalization results for PVRP-P at large sizes and agent numbers. Highlighting cost (\downarrow) and average gaps (\downarrow) to the sota HGS-PyVRP. Single instance solution time in (·).

<i>N</i>	200				500				1000			Gap(%)
<i>M</i>	6	10	14	15	25	35	30	50	70	avg.		
OR-Tools	17.74 (15m)	19.80 (15m)	20.61 (15m)	54.15 (15m)	55.16 (15m)	58.34 (15m)	107.40 (15m)	110.32 (15m)	113.24 (15m)	40.23		
	16.73 (15m)	17.32 (15m)	18.24 (15m)	35.67 (15m)	37.05 (15m)	38.60 (15m)	64.70 (15m)	70.86 (15m)	72.94 (15m)	0.00		
ET (g.)	31.10 (0.51s)	31.12 (0.53s)	31.35 (0.59s)	80.54 (1.12s)	80.32 (1.10s)	80.98 (1.17s)	146.08 (2.11s)	153.62 (2.41s)	153.02 (2.51s)	104.68		
DPN (g.)	27.04 (0.51s)	27.06 (0.53s)	27.26 (0.59s)	70.04 (1.12s)	69.84 (1.10s)	70.42 (1.17s)	127.03 (2.11s)	133.58 (2.41s)	133.06 (2.51s)	77.98		
2D-Ptr (g.)	23.82 (0.32s)	23.58 (0.35s)	24.23 (0.37s)	57.77 (0.60s)	57.60 (0.59s)	57.85 (0.62s)	104.78 (1.02s)	110.16 (1.11s)	109.32 (1.07s)	49.55		
PARCO (g.)	21.20 (0.38s)	20.99 (0.39s)	21.56 (0.42s)	51.41 (0.63s)	51.26 (0.66s)	51.49 (0.70s)	93.25 (1.19s)	98.05 (1.23s)	97.29 (1.29s)	33.10		
CAMP (g.)	20.83 (0.41s)	20.62 (0.43s)	21.19 (0.46s)	50.51 (0.69s)	50.37 (0.72s)	50.59 (0.76s)	91.62 (1.27s)	96.33 (1.33s)	95.59 (1.38s)	30.77		
USPR (g.)	19.81 (0.33s)	19.61 (0.34s)	20.15 (0.37s)	48.04 (0.57s)	47.90 (0.59s)	48.11 (0.62s)	87.13 (1.01s)	91.61 (1.08s)	90.91 (1.12s)	24.36		
ET (s.)	30.47 (0.55s)	30.50 (0.60s)	30.72 (0.65s)	78.93 (1.23s)	78.71 (1.26s)	79.36 (1.31s)	143.16 (2.48s)	150.54 (2.58s)	149.96 (2.70s)	100.59		
DPN (s.)	23.99 (0.56s)	24.00 (0.59s)	23.96 (0.65s)	64.71 (1.24s)	65.20 (1.21s)	66.23 (1.29s)	117.37 (2.32s)	124.69 (2.66s)	125.14 (2.78s)	63.46		
2D-Ptr (s.)	21.14 (0.36s)	20.91 (0.38s)	21.30 (0.41s)	53.38 (0.66s)	53.77 (0.65s)	54.41 (0.69s)	96.81 (1.12s)	102.83 (1.22s)	102.81 (1.19s)	37.24		
PARCO (s.)	20.78 (0.42s)	20.57 (0.43s)	21.13 (0.46s)	50.39 (0.70s)	50.24 (0.73s)	50.46 (0.77s)	91.39 (1.32s)	96.08 (1.36s)	95.35 (1.42s)	30.44		
CAMP (s.)	20.47 (0.43s)	20.27 (0.46s)	20.82 (0.48s)	49.64 (0.74s)	49.50 (0.79s)	49.71 (0.81s)	90.04 (1.34s)	94.67 (1.45s)	93.94 (1.49s)	28.51		
USPR (s.)	18.85 (0.37s)	18.66 (0.38s)	19.17 (0.41s)	45.70 (0.63s)	45.57 (0.65s)	45.77 (0.69s)	82.89 (1.12s)	87.16 (1.19s)	86.49 (1.24s)	18.32		

Testing Protocol We consider three main settings for evaluating USPR. Firstly, we consider in-distribution results, where we evaluate each model on 1,280 randomly generated instances per profile type, covering all combinations of client counts $N \in \{60, 80, 100\}$ and vehicle counts $M \in \{3, 5, 7\}$. Secondly, we test 16 instances in out-of-distribution generalization, with vehicle numbers $M \in \{6, 10, 14\}$ for $N = 200$, $M \in \{15, 25, 35\}$ for $N = 500$, and $M \in \{30, 50, 70\}$ for $N = 1000$ with vehicle capacity $Q_k = 30 + \lfloor \frac{N}{5} \rfloor$ which is commonly used in NCO for VRP approaches [33, 31]. We finally introduce a variation of the real-world data of CVRP1_ib², which we coin *PVRPLib*, which is based on the number

of vehicles, capacity values, and coordinates of the original CVR-PLib but with profiles generated as described in the data generation paragraph. For each instance, we measure both greedy performance ($g.$), i.e., taking the arg max over decoder log-probabilities, and sampling 1,280 solutions per instance ($s.$). Final performance metrics are reported as averages over all profile distributions and α settings.

5.2 Main Results

In-distribution Performance Table 1 shows a comparison between our method and the baseline models on the PVRP-P and PVRP-ZC, with inference times indicated in parentheses (·). The results demonstrate that our USPR achieves state-of-the-art perfor-

² <http://vrp.atd-lab.inf.puc-rio.br/index.php/en/>

mance for all problem settings, consistently outperforming all existing neural solvers in both solution quality and computational efficiency, as well as outperforming Google OR-Tools (both with greedy and sampling performance) while at a fraction of the computational cost. Notably, unlike previous approaches that require training separate models for different problem types and preference weights, USPR is trained as a single unified model, effectively handling varying client-vehicle constraints and preference distributions within a single framework.

Out-of-Distribution Performance We test USPR with out-of-distribution performance in [Table 2](#), particularly in large scales – up to $10 \times$ the number of agents M and $10 \times$ the number of nodes N . Our model outperforms all previous neural methods. Autoregressive methods ET and DPN quickly degrade in performance due to their inability to handle long sequences with a single agent at a time, uninformed of peer agents’ decisions. We observe that parallel autoregressive methods PARCO, CAMP and ours perform on average better than OR-Tools, and that the improvement of USPR and previous SOTA CAMP widens for large-scale out-of-distribution settings, which we attribute to our method’s superior profile handling.

Table 3. Gap comparison of different methods across PVRPLib instances. The best-known solutions (BKS) are collected by HGS-PyVRP.

Dataset	Size	BKS	CAMP		USPR	
			Cost	Gap	Cost	Gap
Set A	31-79	9.24	9.87	6.82%	9.72	5.19%
Set B	30-77	10.18	10.80	6.09%	10.71	5.21%
Set F	44-134	12.68	13.58	7.10%	13.52	6.62%
Set M	100-199	45.63	54.39	19.20%	51.77	13.46%
Set P	15-100	9.09	9.67	6.38%	9.55	5.06%
Set X	100-300	15.56	19.01	22.17%	17.98	15.55%
	300-500	38.08	48.98	28.62%	46.12	21.11%
	500-700	66.04	95.67	44.87%	82.18	24.44%
	700-1000	99.08	136.71	38.00%	126.64	27.82%

Real-world Settings We further analyze the performance of USPR against the SOTA neural method CAMP on the newly proposed PVRPLib, containing real-world location distributions, demands, number of vehicles, and the added preferences in [Table 3](#). Our method remarkably improves on CAMP by 24% on average.

5.3 Analysis

Ablation Study We perform an ablation study on PVRP-P to evaluate the contribution of model components in [Fig. 3](#).

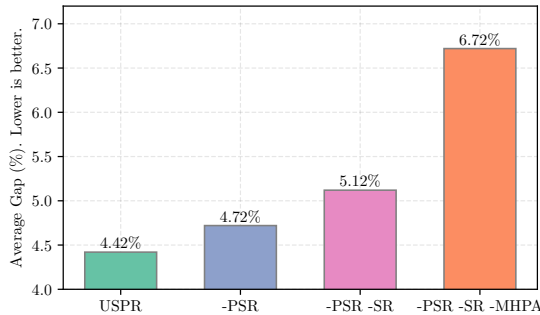


Figure 3. Ablation study for our model showing gaps (\downarrow) removing different components on PVRP-P.

We remove both the full PSR from [Section 4.3](#) – i.e., removing $-\log(\text{dist}_{ij} + p_{ij})$ – and SR (distance only) – i.e., keeping only the

score reshaping for the distance $-\log(\text{dist}_{ij})$ akin to Huang et al. [25]. We note that removing the attention score reshaping altogether degrades the performance, where we note that the inclusion of profile in PSR is important for performance improvements. The most significant drop occurs when eliminating the MHPA, highlighting its critical role in improving inter-agent communication and capturing profile-specific interactions.

Training Time Savings We showcase in [Table 4](#) highlights the efficiency of our unified model compared to single-task CAMP.

Table 4. Our unified model enables substantial memory and training time savings compared to single-task CAMP.

	# Models	# Total Param.	# Total Epochs	Train Time
CAMP	10	17.6M	1000	4.6 days
USPR	1	1.5M	100	11 hours

We significantly reduce memory and computational costs by utilizing a single model instead of 10, cutting total parameters from 17.6M to 1.5M and training time from 4.6 days to just 11 hours. Additionally, our model requires only 100 epochs, an order of magnitude fewer than CAMP’s 1000, while maintaining competitive performance. This efficiency aligns with our goal of a scalable and adaptable solution for PVRP, eliminating the need for training separate models while ensuring high-quality optimization across diverse vehicle-client profiles.

Effect of α With increasing α , our model shifts focus towards profile adherence while maintaining strong duration optimization (see [Eq. \(1\)](#)), effectively capturing vehicle-client interactions. A single unified model is used to solve for any value of α as input to the Profile Embeddings. [Fig. 4](#) shows USPR solutions for different values of α , demonstrating how increasing its value makes the model trade-off duration for overall profiles adherence – preferences in this case. This makes our model highly scalable and adaptable for real-world applications.

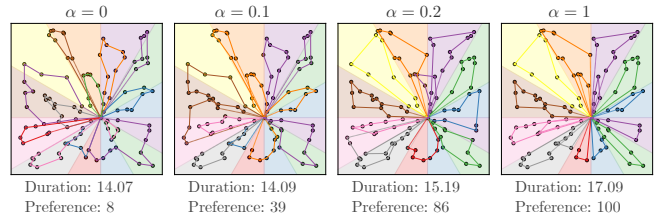


Figure 4. USPR’s PVRP solutions to the same instance with different α processed through the Profile Embeddings. A higher α favors adherence to profile values, while $\alpha = 0$ converts the problem to a classical VRP.

6 Conclusion

In this work, we introduced USPR (Unified Solver for Profiled Routing), a learning-based framework that addresses the key limitations of existing PVRP neural solvers through three novel components: Profile Embeddings (PE) for encoding arbitrary profile distributions, Multi-Head Profiled Attention (MHPA) for modeling rich vehicle-client interactions, and Profile-aware Score Reshaping (PSR) for robust generalization. Our comprehensive experiments demonstrate that USPR consistently outperforms state-of-the-art neural methods across both preference-based and zone-constrained routing problems, while matching or exceeding classical solvers at significantly lower computational cost. Notably, a single USPR model effectively handles varying profile weights and generalizes to out-of-distribution

instances up to $10\times$ larger than training data, eliminating the need for multiple specialized models. By providing this unified approach to profiled routing optimization and making our implementation publicly available, we aim to advance neural combinatorial optimization research and enable more flexible, efficient solutions for complex routing problems in real-world logistics operations.

References

- [1] S. AIKO, P. THAITHATKUL, and Y. Asakura. Incorporating user preference into optimal vehicle routing problem of integrated sharing transport system. *Asian Transport Studies*, 5(1):98–116, 2018.
- [2] A. Bdeir, J. K. Falkner, and L. Schmidt-Thieme. Attention, filling in the gaps for generalization in routing problems. In *ECML PKDD*, pages 505–520. Springer, 2022.
- [3] I. Bello, H. Pham, Q. V. Le, M. Norouzi, and S. Bengio. Neural combinatorial optimization with reinforcement learning. *arXiv preprint arXiv:1611.09940*, 2016.
- [4] Y. Bengio, A. Lodi, and A. Prouvost. Machine learning for combinatorial optimization: a methodological tour d’horizon. *European Journal of Operational Research*, 290(2):405–421, 2021.
- [5] F. Berto, C. Hua, L. Luttmann, J. Son, J. Park, K. Ahn, C. Kwon, L. Xie, and J. Park. PARCO: Learning Parallel Autoregressive Policies for Efficient Multi-Agent Combinatorial Optimization. *arXiv preprint arXiv:2409.03811*, 2024.
- [6] F. Berto, C. Hua, J. Park, L. Luttmann, Y. Ma, F. Bu, J. Wang, H. Ye, M. Kim, S. Choi, N. G. Zepeda, A. Hottung, J. Zhou, J. Bi, Y. Hu, F. Liu, H. Kim, J. Son, H. Kim, D. Angioni, W. Kool, Z. Cao, J. Zhang, K. Shin, C. Wu, S. Ahn, G. Song, C. Kwon, L. Xie, and J. Park. RL4CO: an Extensive Reinforcement Learning for Combinatorial Optimization Benchmark. *arXiv preprint arXiv:2306.17100*, 2024.
- [7] F. Berto, C. Hua, N. G. Zepeda, A. Hottung, N. Wouda, L. Lan, K. Tierney, and J. Park. RouteFinder: Towards foundation models for vehicle routing problems. In *ICML 2024 FM-Wild Workshop*, 2024.
- [8] J. Bi, Y. Ma, J. Zhou, W. Song, Z. Cao, Y. Wu, and J. Zhang. Learning to handle complex constraints for vehicle routing problems. *arXiv preprint arXiv:2410.21066*, 2024.
- [9] A. Bogrybayeva, T. Yoon, H. Ko, S. Lim, H. Yun, and C. Kwon. A deep reinforcement learning approach for solving the traveling salesman problem with drone. *Transportation Research Part C: Emerging Technologies*, 148:103981, 2023.
- [10] K. Braekers, K. Ramaekers, and I. Van Nieuwenhuyse. The vehicle routing problem: State of the art classification and review. *Computers & industrial engineering*, 99:300–313, 2016.
- [11] J. Choo, Y.-D. Kwon, J. Kim, J. Jae, A. Hottung, K. Tierney, and Y. Gwon. Simulation-guided beam search for neural combinatorial optimization. *NeurIPS*, 35:8760–8772, 2022.
- [12] J.-F. Cordeau and G. Laporte. A tabu search heuristic for the site dependent vehicle routing problem with time windows. *INFOR*, 39(4):292–298, 2001.
- [13] D. Drakulic, S. Michel, F. Mai, A. Sors, and J.-M. Andreoli. Bq-nco: Bisimulation quotienting for efficient neural combinatorial optimization. *NeurIPS*, 36, 2024.
- [14] D. Drakulic, S. Michel, and J.-M. Andreoli. Goal: A generalist combinatorial optimization agent learning. In *ICLR*, 2025.
- [15] L. Duan, Y. Zhan, H. Hu, Y. Gong, J. Wei, X. Zhang, and Y. Xu. Efficiently Solving the Practical Vehicle Routing Problem: A Novel Joint Learning Approach. In *KDD*. ACM, 2020.
- [16] Y. L. Goh, Y. Ma, J. Zhou, Z. Cao, M. H. Dupty, and W. S. Lee. Shield: Multi-task multi-distribution vehicle routing solver with sparsity & hierarchy in efficiently layered decoder. In *ICML*, 2025.
- [17] B. Golden, A. Assad, L. Levy, and F. Gheysens. The fleet size and mix vehicle routing problem. *Computers & Operations Research*, 11(1):49–66, 1984.
- [18] N. Grinsztajn, D. Furelos-Blanco, S. Surana, C. Bonnet, and T. Barrett. Winner takes it all: Training performant rl populations for combinatorial optimization. *NeurIPS*, 36:48485–48509, 2023.
- [19] N. Grinsztajn, D. Furelos-Blanco, S. Surana, C. Bonnet, and T. Barrett. Winner takes it all: Training performant rl populations for combinatorial optimization. *NeurIPS*, 36, 2024.
- [20] A. Hottung and K. Tierney. Neural large neighborhood search for the capacitated vehicle routing problem. In *ECAI 2020*. IOS Press, 2020.
- [21] A. Hottung, Y.-D. Kwon, and K. Tierney. Efficient active search for combinatorial optimization problems. In *ICLR*, 2022.
- [22] A. Hottung, M. Mahajan, and K. Tierney. PolyNet: Learning diverse solution strategies for neural combinatorial optimization. *ICLR*, 2025.
- [23] A. Hottung, P. Wong-Chung, and K. Tierney. Neural deconstruction search for vehicle routing problems. *TMLR*, 2025.
- [24] C. Hua, F. Berto, J. Son, S. Kang, C. Kwon, and J. Park. CAMP: Collaborative Attention Model with Profiles for Vehicle Routing Problems. In *AAMAS*, 2025.
- [25] Z. Huang, J. Zhou, Z. Cao, and Y. Xu. Rethinking light decoder-based solvers for vehicle routing problems. *arXiv preprint arXiv:2503.00753*, 2025.
- [26] D. S. Johnson and L. A. McGeoch. The traveling salesman problem: a case study. *Local search in combinatorial optimization*, 1997.
- [27] H. Kim, S. Choi, J. Son, J. Park, and C. Kwon. Neural genetic search in discrete spaces. *arXiv preprint arXiv:2502.10433*, 2025.
- [28] M. Kim, J. Park, and J. Park. Sym-nco: Leveraging symmetry for neural combinatorial optimization. *NeurIPS*, 35:1936–1949, 2022.
- [29] M. Kim, S. Choi, J. Son, H. Kim, J. Park, and Y. Bengio. Ant colony sampling with glownets for combinatorial optimization. *arXiv preprint arXiv:2403.07041*, 2024.
- [30] D. P. Kingma and J. Ba. Adam: A method for stochastic optimization. *arXiv preprint arXiv:1412.6980*, 2014.
- [31] W. Kool, H. Van Hoof, and M. Welling. Attention, learn to solve routing problems! *arXiv preprint arXiv:1803.08475*, 2018.
- [32] W. Kool, H. van Hoof, J. Gromicho, and M. Welling. Deep policy dynamic programming for vehicle routing problems. In *CRAIOP*, pages 190–213. Springer, 2022.
- [33] Y.-D. Kwon, J. Choo, B. Kim, I. Yoon, Y. Gwon, and S. Min. Pomo: Policy optimization with multiple optima for reinforcement learning. *NeurIPS*, 33:21188–21198, 2020.
- [34] H. Li, F. Liu, Z. Zheng, Y. Zhang, and Z. Wang. Cada: Cross-problem routing solver with constraint-aware dual-attention. *arXiv preprint arXiv:2412.00346*, 2024.
- [35] J. Li, Y. Ma, R. Gao, Z. Cao, A. Lim, W. Song, and J. Zhang. Deep reinforcement learning for solving the heterogeneous capacitated vehicle routing problem. *IEEE Transactions on Cybernetics*, 2022.
- [36] S. Li, Z. Yan, and C. Wu. Learning to delegate for large-scale vehicle routing. *NeurIPS*, 34:26198–26211, 2021.
- [37] Y. Li, C. Zhou, P. Yuan, and T. T. A. Ngo. Experience-based territory planning and driver assignment with predicted demand and driver present condition. *Transportation research part E: logistics and transportation review*, 171:103036, 2023.
- [38] Y. Li, J. Guo, R. Wang, and J. Yan. From distribution learning in training to gradient search in testing for combinatorial optimization. *NeurIPS*, 36, 2024.
- [39] Y. Li, J. Ma, W. Pan, R. Wang, H. Geng, N. Yang, and J. Yan. Unify ml4tsp: Drawing methodological principles for tsp and beyond from streamlined design space of learning and search. In *The Thirteenth International Conference on Learning Representations*, 2025.
- [40] F. Liu, X. Lin, Z. Wang, Q. Zhang, T. Xialiang, and M. Yuan. Multi-task learning for routing problem with cross-problem zero-shot generalization. In *KDD*, 2024.
- [41] F. Liu, T. Xialiang, M. Yuan, X. Lin, F. Luo, Z. Wang, Z. Lu, and Q. Zhang. Evolution of heuristics: Towards efficient automatic algorithm design using large language model. In *ICML*, 2024.
- [42] Q. Liu, C. Liu, S. Niu, C. Long, J. Zhang, and M. Xu. 2d-ptr: 2d array pointer network for solving the heterogeneous capacitated vehicle routing problem. In *AAMAS*, pages 1238–1246, 2024.
- [43] M. Lozano, D. Molina, and F. Herrera. Editorial scalability of evolutionary algorithms and other metaheuristics for large-scale continuous optimization problems. *Soft computing*, 15:2085–2087, 2011.
- [44] Y. Ma, Z. Cao, and Y. M. Chee. Learning to search feasible and infeasible regions of routing problems with flexible neural k-opt. *NeurIPS*, 36, 2024.
- [45] N. Mazyavkina, S. Sviridov, S. Ivanov, and E. Burnaev. Reinforcement learning for combinatorial optimization: A survey. *Computers & Operations Research*, 134:105400, 2021.
- [46] W. Ouyang, S. Li, Y. Ma, and C. Wu. Learning to segment for capacitated vehicle routing problems. 2025.
- [47] C. H. Papadimitriou and K. Steiglitz. *Combinatorial optimization: algorithms and complexity*. Courier Corporation, 1998.
- [48] L. Perron and V. Furnon. *OR-Tools*. Google, 2023.
- [49] V. T. D. Pham, L. Doan, and T. T. B. Huynh. HSEvo: Elevating Automatic Heuristic Design with Diversity-Driven Harmony Search and Genetic Algorithm Using LLMs. In *AAAI*. Association for the Advancement of Artificial Intelligence (AAAI), 2025.
- [50] J. Pirnay and D. G. Grimm. Take a step and reconsider: Sequence decoding for self-improved neural combinatorial optimization. In *ECAI*, 2024.
- [51] J. Son, M. Kim, S. Choi, H. Kim, and J. Park. Equity-transformer: Solving np-hard min-max routing problems as sequential generation with

equity context. In *AAAI*, 2024.

[52] J. Son, Z. Zhao, F. Berto, C. Hua, C. Kwon, and J. Park. Neural combinatorial optimization for real-world routing. *arXiv preprint arXiv:2503.16159*, 2025.

[53] Z. Sun and Y. Yang. Difusco: Graph-based diffusion solvers for combinatorial optimization. *NeurIPS*, 36, 2024.

[54] Z. Sun, Z. Li, H. Wang, D. He, Z. Lin, and Z. Deng. Fast structured decoding for sequence models. *NeurIPS*, 32, 2019.

[55] H. Tang, F. Berto, Z. Ma, C. Hua, K. Ahn, and J. Park. Himap: Learning heuristics-informed policies for large-scale multi-agent pathfinding. *arXiv preprint arXiv:2402.15546*, 2024.

[56] H. Tang, F. Berto, and J. Park. Ensembling prioritized hybrid policies for multi-agent pathfinding. In *2024 IEEE/RSJ International Conference on Intelligent Robots and Systems (IROS)*, pages 8047–8054. IEEE, 2024.

[57] Team Locus. Zone-based routing is the need of the hour. *Locus Blog*, 2020. URL <https://www.locus.sh/blog/zone-based-routing-is-the-need-of-the-hour>. Access: 2024-10-17.

[58] C. D. Tran, Q. Nguyen-Tri, H. T. T. Binh, and H. Thanh-Tung. Large language models powered neural solvers for generalized vehicle routing problems. In *Towards Agentic AI for Science: Hypothesis Generation, Comprehension, Quantification, and Validation*.

[59] T. Vidal. Hybrid genetic search for the cvrp: Open-source implementation and swap* neighborhood. *Computers & Operations Research*, 140: 105643, 2022.

[60] O. Vinyals, M. Fortunato, and N. Jaitly. Pointer networks. *NeurIPS*, 28, 2015.

[61] Y. Wang, Y.-H. Jia, W.-N. Chen, and Y. Mei. Distance-aware attention reshaping: Enhance generalization of neural solver for large-scale vehicle routing problems. *arXiv preprint arXiv:2401.06979*, 2024.

[62] N. A. Wouda, L. Lan, and W. Kool. PyVRP: A high-performance VRP solver package. *INFORMS Journal on Computing*, 2024.

[63] H. Ye, J. Wang, Z. Cao, H. Liang, and Y. Li. Deepaco: Neural-enhanced ant systems for combinatorial optimization. In *NeurIPS*, 2023.

[64] H. Ye, J. Wang, Z. Cao, F. Berto, C. Hua, H. Kim, J. Park, and G. Song. Reevo: Large language models as hyper-heuristics with reflective evolution. In *NeurIPS*, 2024.

[65] N. Zhang, J. Yang, Z. Cao, and X. Chi. Adversarial generative flow network for solving vehicle routing problems. *arXiv preprint arXiv:2503.01931*, 2025.

[66] Z. Zhao, C. Hua, F. Berto, K. Lee, Z. Ma, J. Li, and J. Park. Trajevo: Designing trajectory prediction heuristics via llm-driven evolution, 2025. URL <https://arxiv.org/abs/2505.04480>.

[67] Z. Zheng, S. Yao, Z. Wang, T. Xialiang, M. Yuan, and K. Tang. DPN: Decoupling partition and navigation for neural solvers of min-max vehicle routing problems. In *ICML*, 2024.

[68] H. Zhong, R. W. Hall, and M. Dessouky. Territory planning and vehicle dispatching with driver learning. *Transportation Science*, 2007.

[69] J. Zhou, Z. Cao, Y. Wu, W. Song, Y. Ma, J. Zhang, and C. Xu. Mvmoe: Multi-task vehicle routing solver with mixture-of-experts. In *ICML*, 2024.

[70] Z. Zong, M. Zheng, Y. Li, and D. Jin. Mapdp: Cooperative multi-agent reinforcement learning to solve pickup and delivery problems. In *AAAI*, 2022.